ELSEVIER

Ceramics International 25 (1999) 115–123

CERAMICS INTERNATIONAL

Bi_2O_3 as an effective sintering aid for $La(Sr)MnO_3$ powder prepared by autoignition route

Amitava Chakraborty *, Himadri S. Maiti

Electroceramics Laboratory, Central Glass and Ceramic Research Institute, Calcutta-700 032, India

Received 9 June 1997; accepted 8 January 1998

Abstract

Sintering characteristics of the Sr-doped lanthanum manganite [$La(Sr)MnO_3$] powder, prepared by autoignition of citrate–nitrate gel, have been studied by measuring density and evaluation of microstructural information. Bi_2O_3 is found to be an effective sintering aid for this material. Increased concentration of point defects arising from substitution of Bi in La site is the plausible cause of enhanced sintering. Measurement of electrical conductivity and thermal expansion coefficient indicate that Bi_2O_3 addition does not have any significant effect on these properties.

Keywords: B. Microstructure; Lanthanum manganite; Sintering aid; Point defect

1. Introduction

Sr-doped lanthanum manganite [$La(Sr)MnO_3$] has been found to be a very promising material in modern ceramics due to its electronic, magnetic and catalytic properties [1–5]. Though several of the bulk properties of $La(Sr)MnO_3$, e.g., the electrical conductivity, are related to sintered density and microstructure of the material [6], the data available on the sintering behaviour of pure and substituted $LaMnO_3$ are limited [7–9]. Van Roosmalen et al. [7] have asserted that the dominating effect in the sinter behaviour of alkaline earth substituted $LaMnO_3$ is (bulk) ionic diffusion. In a recent study, Stevenson et al. [9] showed that the diffusion of A-site cations is the limiting factor in the mass transport during densification.

Additives are commonly used to enhance the densification of a powder compact, with a given particle size and morphology of the powder. These additives either go into solid solution with the host material and form point defects and thereby increases the solid state diffusion rate of the slower moving species or form a reactive liquid phase which flows in between the grains forming a stronger bond. In an earlier study [10], Bi_2O_3 was used as a sintering aid for the material but the information published on this matter is meagre. The compound is also known to be a good sintering aid for lithium ferrite [11]. Since Bi_2O_3 is a good ionic conductor and has a relatively low melting point, it has also been used in the present investigation and an attempt has been made to understand the mechanism by which the enhancement in densification takes place. Sr-doped $LaMnO_3$ (with nominal composition of $La_{0.84}Sr_{0.16}MnO_3$) has been prepared by autoignition of citrate-nitrate gel [12–14]. Addition of small amounts of Bi_2O_3 to this powder is found to have a much stronger effect so far as lowering of sintering temperature and enhanced densification are concerned compared to the powder prepared by conventional solid state reaction route. The electrical conductivity and thermal expansion of the material have also been measured in order to examine the effect of the additive on these properties if any.

2. Experimental

The $La(Sr)MnO_3$ powder has been synthesized by autoignition of citrate–nitrate gel, the details of which are published elsewhere [12–14]. The average particle size of the powder used in this investigation was 1.14 μm. Varying amounts of Bi_2O_3 (1 to 10 wt%) were mixed thoroughly with the powder prepared by

* Corresponding author. Tel.: +91-021-7787; Fax: +91-033-473-0957.

0272-8842/99/$—see front matter
PII: S0272-8842(98)00010-8

autoignition route. The mixture was ball milled in isopropanol medium overnight with subsequent drying and then compacted in the form of small pellets using a pressure of 226 MPa. The pressed samples were sintered in air at different temperatures upto a maximum of 1425°C for 1 to 24 h. Both heating and cooling rates were fixed at 100°C h^{-1}. In a subsequent experiment Bi has been introduced in the precursor mixture of the autoignited system as a component of the final oxide replacing either lanthanum or manganese. In one set of samples 10 at% of Bi was substituted for La in the basic composition $La_{0.84}Sr_{0.16}MnO_3$ which is hereafter termed as composition LA(BI). In the other case, 10 at% of Bi was substituted for Mn in the same basic composition which is to be designated as composition MN(BI). Accordingly, the nominal compositions were $(La_{0.74}Sr_{0.16}Bi_{0.10})MnO_3$ and $(La_{0.84}Sr_{0.16})(Mn_{0.90}Bi_{0.10})O_3$ for LA(BI) and MN(BI) samples, respectively.

Identification of various phases of the powder and sintered samples was carried out by X-ray diffraction analysis in a Philips PW 1730 diffractometer using CuK_α radiation. Differential Thermal Analysis was carried out for the powder with 10 wt% Bi_2O_3 in the temperature range 30–1000°C in static air. The heating rate was maintained at 2°C min^{-1}. The Bulk density of all the sintered samples was measured by liquid displacement method using toluene. Fractured surfaces of the sintered specimens were examined in SEM (Stereo Scan S-250, USA). EPMA study of the polished surface of the sintered materials have been carried out using Camebax-Micro analyser.

The electrical conductivity of the material has been studied from 30–1000°C by standard four probe technique. The thermal expansion has been measured in the temperature range 30–1000°C on cylindrical rods of the sintered samples using a dilatometer (BAHR 804) with a heating rate of 5°C min^{-1}.

3. Results and discussion

3.1. Influence of sintering aid

The effect of Bi_2O_3 on densification of the representative composition $La_{0.84}Sr_{0.16}MnO_3$ is clearly evident from Fig. 1, in which percent theoretical density is plotted against sintering temperature. For all of the samples the extent of sintering is negligible below 800°C. In the absence of Bi_2O_3 the densification increases very slowly with increasing temperature. Very little sintering takes place below 1050°C and a maximum of around 88% densification occurs at a sintering temperature of 1350°C. But with addition of only 1 wt% Bi_2O_3 there is a sudden increase in density between 1050 and 1125°C, thereafter it increases rather gradually till about 1275°C. For enhancing the sintering rate, 10 wt% Bi_2O_3 addition is still more effective, particularly at lower temperatures. In this case the maximum rate of densification is observed between 900 and 1050°C and a density >93% of the theoretical value is achieved at a temperature as low as 1200°C. These results clearly show the effectiveness of bismuth oxide as a sintering aid for the material. It has been further observed from the sintering curves that the sintered density decreases at high temperatures. This is attributed to the evaporation of some bismuth during high temperature sintering as confirmed from chemical analysis (Table 1). Above 1350°C some loss of manganese also takes place.

The effectiveness of Bi_2O_3 as a sintering aid is also evident from the SEM fractographs of the sintered specimens presented in Fig. 2(a)–(d). A progressive change in microstructure with Bi_2O_3 content is clearly visible. As expected, more and more dense microstructure is formed with increasing Bi_2O_3 content. A highly dense clean microstructure with faceted grains is formed with the highest amount of Bi_2O_3. No separate grain boundary phase appears to be formed during sintering.

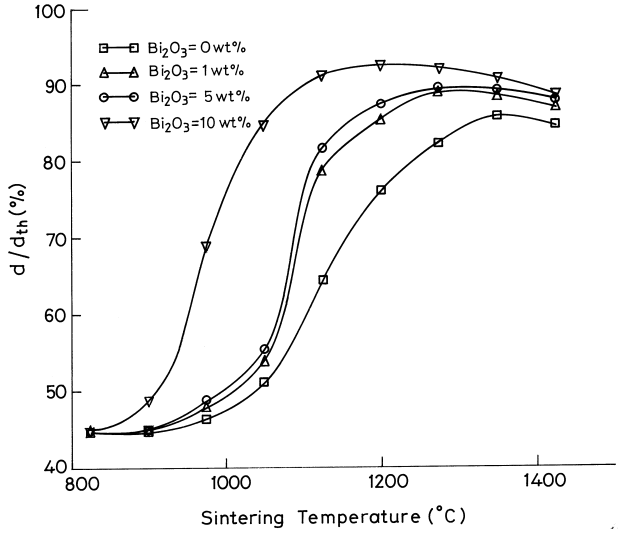

Fig. 1. Effect of sintering temperature on densification for $La_{0.84}Sr_{0.16}MnO_3$ prepared by autoignition technique (average particle size 1.14 μm) containing different wt% of Bi_2O_3 (sintering time 6 h).

Table 1
Chemical analysis of the sintered (1200°C for 6 h) samples of Bi_2O_3 added $La_{0.84}Sr_{0.16}MnO_3$

Bi_2O_3 to the nominal composition (wt%)	Amount of Bi expected in the nominal composition (wt%)	Amount of Bi present after sintering at 1200°C 6 h (wt%)
1	0.897	0.870
5	4.485	4.200
10	8.890	8.090

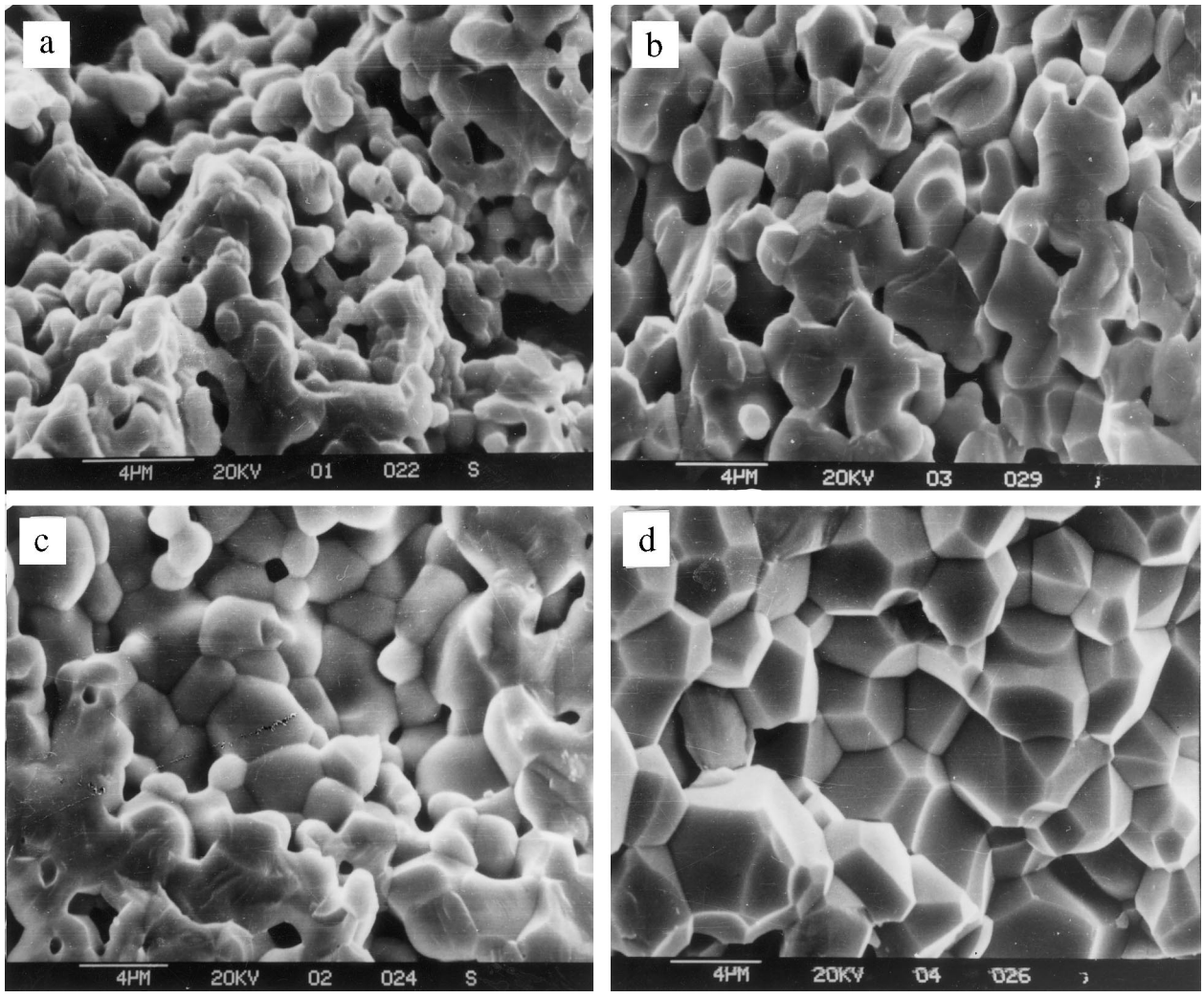

Fig. 2. SEM photographs of fractured surface of the sintered (1200°C for 6 h) sample of $La_{0.84}Sr_{01.16}MnO_3$, prepared by autoignition technique, containing different wt% of Bi_2O_3: (a) 0, (b) 1, (c) 5 and (d) 10.

It has also been observed from XRD study that with up to 10 wt% addition of Bi_2O_3 in La(Sr)MnO_3 a complete solid solution is formed (disappearance of the Bi_2O_3 peaks) when heated to a temperature as low as 800°C (Fig. 3). Since no additional phase containing bismuth has been detected by XRD, it is certain that Bi_2O_3 has entered the lattice of $La_{0.84}Sr_{0.16}MnO_3$ at least partially. Thus, from the X-ray diffraction and SEM study, it is clear that the liquid phase sintering does not appear to be the mechanism for enhanced sintering in this system. This was also verified from the results of the Differential Thermal Analysis of the sample. Even addition of as high as 10 wt% Bi_2O_3 does not show appearance of any sharp endothermic peak due to melting of Bi_2O_3 (Fig. 4) at or near 824°C, the melting point of Bi_2O_3, unlike that observed in the case of liquid phase sintering of lithium ferrite using Bi_2O_3 as a sintering flux [11].

The EPMA study with X-ray mapping of the elements on the polished surface of the above samples sintered at 1200°C show homogeneous distribution of Bi in the La(Sr)MnO3 matrix below 10 wt% of Bi_2O_3 addition in La(Sr)MnO_3 (Fig. 5). Addition of 10 wt% Bi_2O_3 show small amount of Bi segregation takes place at the grain boundaries. This, however, was not detected with the resolution of XRD technique (Fig. 3). So, the actual limit for solubility of Bi_2O_3 in $La_{0.84}Sr_{0.16}MnO_3$ appears to be slightly less than 10 wt%.

The results of chemical analysis for the amount of Bi present in the samples after sintering at 1200°C for 6 h also show that most of the Bi remains in the material and a small portion is evaporated during sintering (Table 1).

Hence, solid state sintering with increased point defect concentration resulting from solid solution effect is the plausible cause of enhanced sintering. The average particle size used in this investigation is 1.14 μm with 46% particles being in the submicron range. The effectiveness of Bi_2O_3 as the sintering aid is observed to be

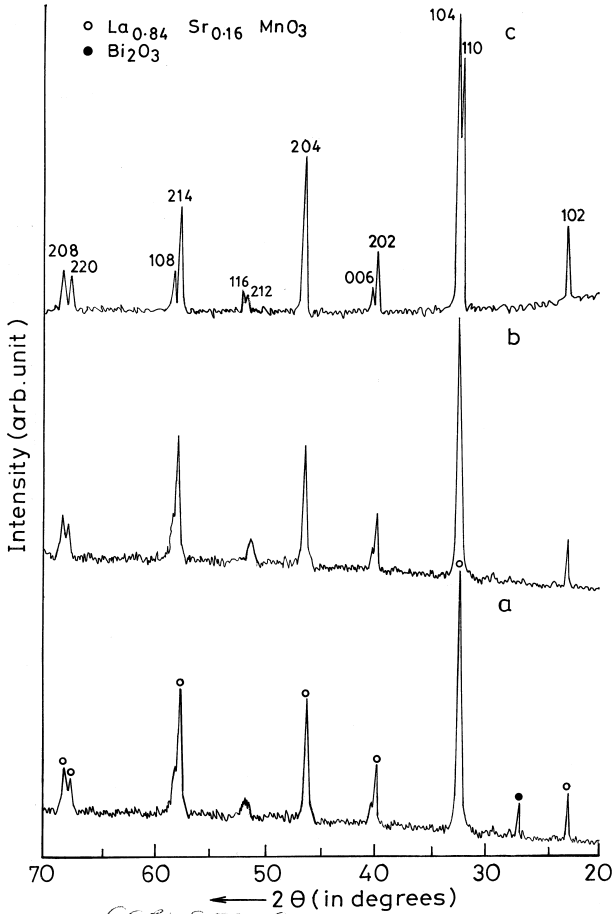

Fig. 3. XRD pattern of $La_{0.84}Sr_{0.16}MnO_3$ with 10 wt% Bi_2O_3 (a) before heat treatment, (b) after sintering at 800°C 6 h and (c) after sintering at 1200°C 6 h.

more significant in this investigation compared to that reported earlier [10] probably due to the finer particle size of the powder used in this work.

3.2. Result of Bi substitution

From X-ray diffraction study it is found that the composition LA(BI), where 10 at% Bi has been substituted for La gives a single phase material with pseudocubic symmetry at a calcination temperature of 850°C and the symmetry changes to haxagonal–rhombohedral at 1200°C (Fig. 6) The particle size at calcination temperature of 850°C is found to be 1.62 μm. On the other hand the composition MN(BI), where 10 at% Bi is substituted for Mn does not give a single phase material even at a calcination temperature of 1250°C (Fig. 7) Apart from the perovskite phase, oxides of bismuth and lanthanum exist as secondary phases in the latter material. Thus it is confirmed that the Bi^{3+} with ionic radius 1.25 Å [15] goes to the La^{3+} (ionic radius 1.46 Å) site instead of entering the Mn^{3+} (ionic radius 0.72 Å) site and produces a single phase material upto 1250°C in case of the composition LA(BI). At 1350°C,

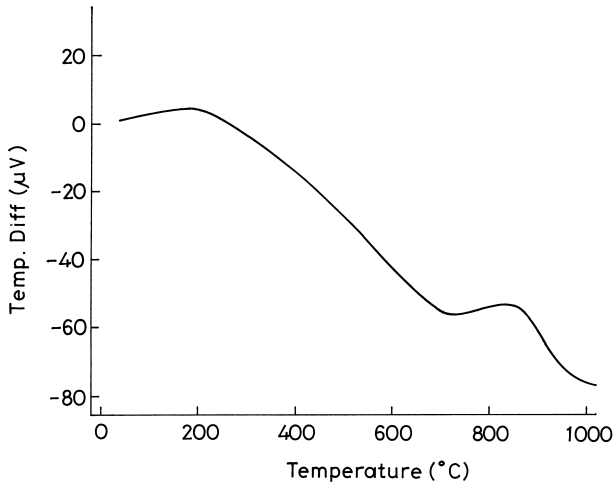

Fig. 4. DTA plot of autoignited $La_{0.84}Sr_{0.16}MnO_3$ powder containing 10 wt% Bi_2O_3.

the composition MN(BI) also gives rise to a single phase material possibly due to evaporation of bismuth containing phases at this temperature.

The variation of sintered density with temperature for the composition LA(BI) and MN(BI) is shown in. Fig. 8 Sintering process for the single phase material LA(BI) is found to be much faster than that for the multiphase material MN(BI). For example, at a temperature of 1200°C the density obtained for the composition LA(BI) is around 90% of the theoretical value compared to that of only 65% in case of composition MN(BI).

From the SEM fractograph (Fig. 9(a) and (b)), it is clearly visible that the composition "LA(BI)" gives a dense microstructure with beautifully developed grains when sintered at 1200°C for 6 h and formation of liquid phase does not appear to be present in the microstructure (Fig. 9(a)). On the other hand the composition MN(BI) does not sinter well at the same temperature (Fig. 9(b)) and shows the formation of liquid phase.

The same feature is also confirmed from EPMA study (Figs. 10(a) and (b)). Homogeneous distribution of the constituting elements (La,Mn, Sr, Bi) is achieved for composition LA(BI) whereas composition MN(BI) clearly shows several bismuth rich regions which have been confirmed as oxides of bismuth from XRD analysis. Thus inspite of the presence of low melting oxides of bismuth in composition MN(BI), the material does not sinter well. Hence, the poor sinterability of this composition once again proves that the liquid phase sintering is not the principal mechanism for this system and solid state sintering plays a greater role in sintering.

3.3. Role of Bi in enhancing the sintering rate

To understand the role of bismuth in enhancing the sintering process in lanthanum manganite a physical

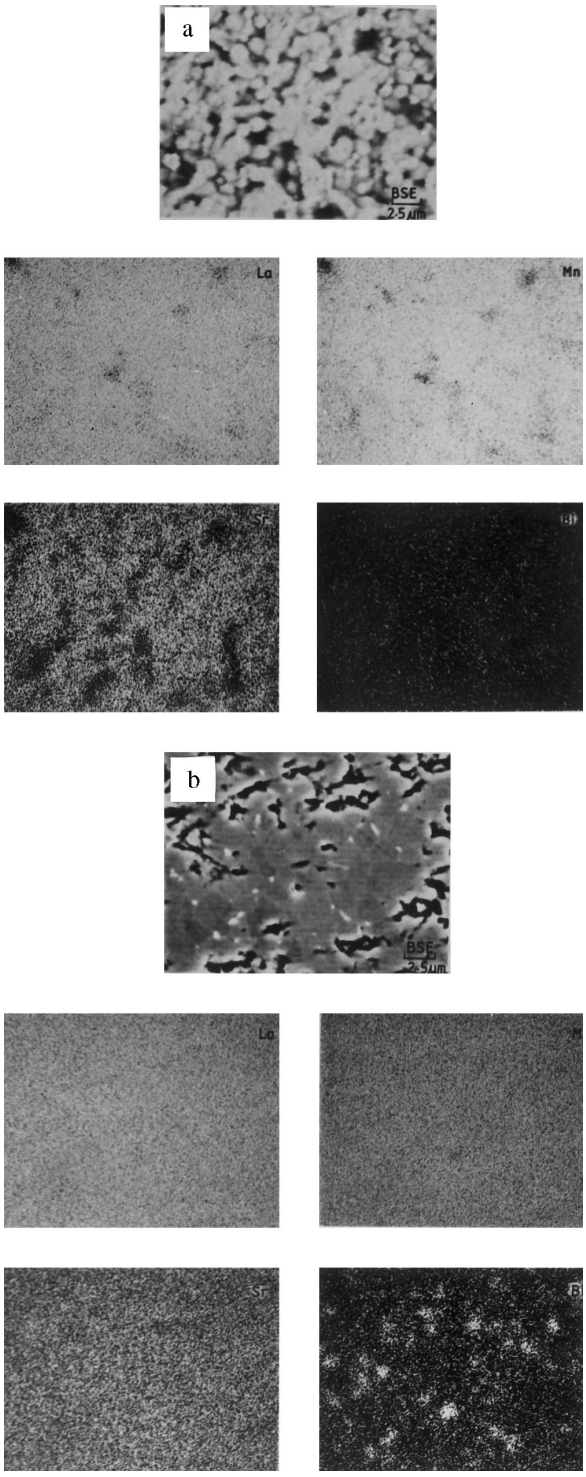

Fig. 5. EPMA photographs showing elemental distribution of the polished surface of sintered (1200°C for 6 h) $La_{0.84}Sr_{0.16}MnO_3$ containing (a) 1 wt% Bi_2O_3 and (b) 10 wt% Bi_2O_3.

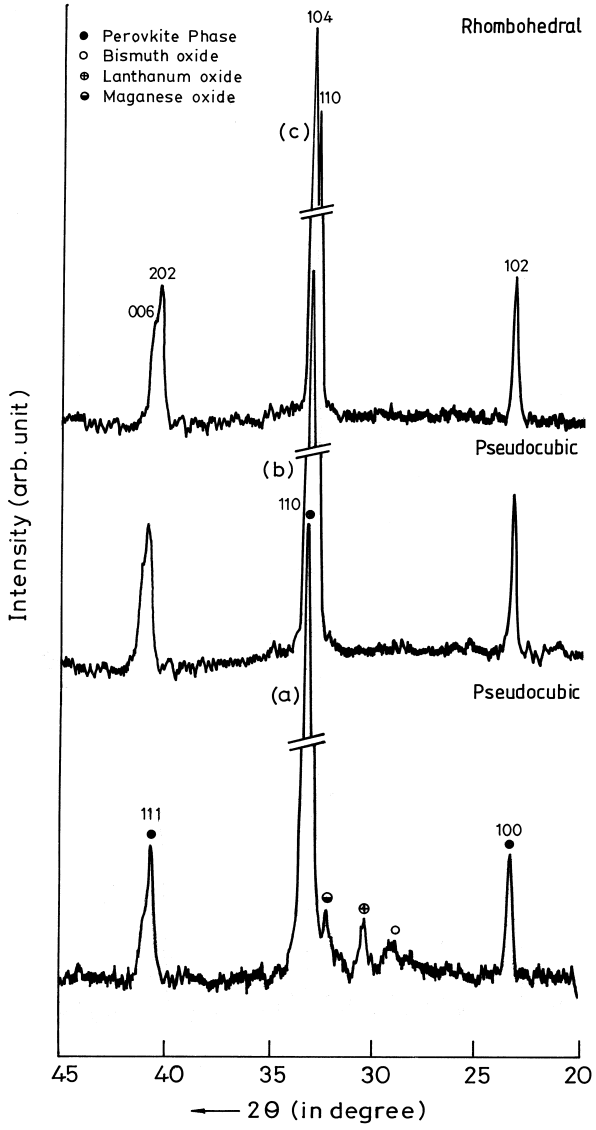

Fig. 6. XRD patterns of the sample LA(BI) calcined at (a) 800°C, (b) 850°C and (c) 1200°C.

model may be proposed. The La_2O_3–Mn_2O_3 phase diagram proposed earlier [16] indicates that the ABO_3 type perovskite compound $LaMnO_3$ is stable over a wide range of La or Mn vacancy. Since Bi^{3+} ions enter into the "A" (La) site, addition of Bi_2O_3 in La(Sr)MnO_3 increases the A:B ratio, i.e., the (La + Sr + Bi):Mn ratio and thereby creating "B" site vacancies in the material. Assuming that all the Bi^{3+} ions go to the La^{3+} site, for addition of 1, 5 and 10 wt% of Bi_2O_3, the A:B ratio in the lattice becomes 1.011, 1.055 and 1.110, respectively. Again at 850°C for Mn ("B" site) vacancy, the material is reported to be stable upto La:Mn ratio of 1.202 [16]. Thus, even with addition of 10 wt% Bi_2O_3 (corresponding to A:B ratio of 1.110), a complete solid solution is formed and the material remains single phase within the calcination temperature of 800°C. La^{3+} and Sr^{2+} (A site) ions with larger ionic radii are reported to be slower moving species than Mn^{3+} or Mn^{4+} (B site) in the compound La(Sr)MnO_3 [7]. Again, diffusivity of Bi^{3+} ion with smaller ionic radius is faster than that of La^{3+} or Sr^{2+} having larger ionic radii. Thus increase in Bi^{3+} ions as a result of addition of Bi_2O_3 increases the overall

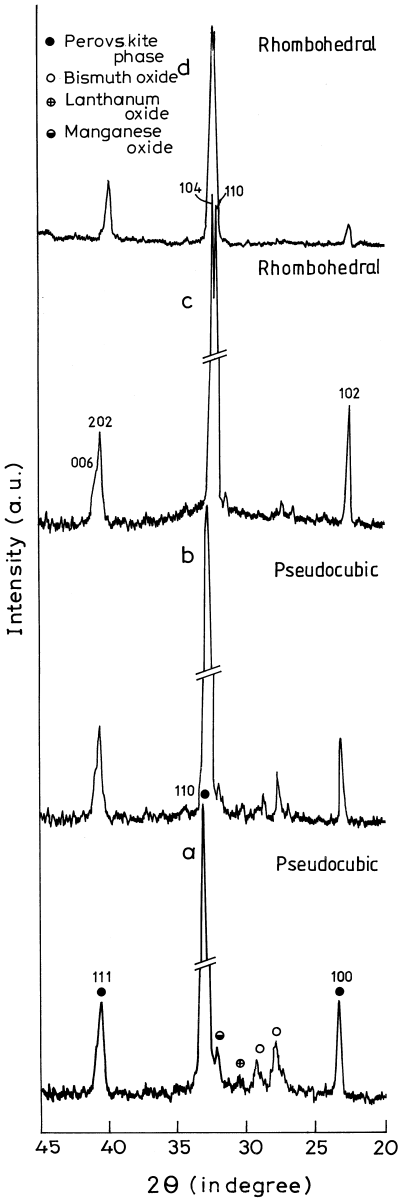

Fig. 7. XRD patterns of the sample MN(BI) calcined at (a) 800°C, (b) 850°C, (c) 1250°C and (d) 1350°C.

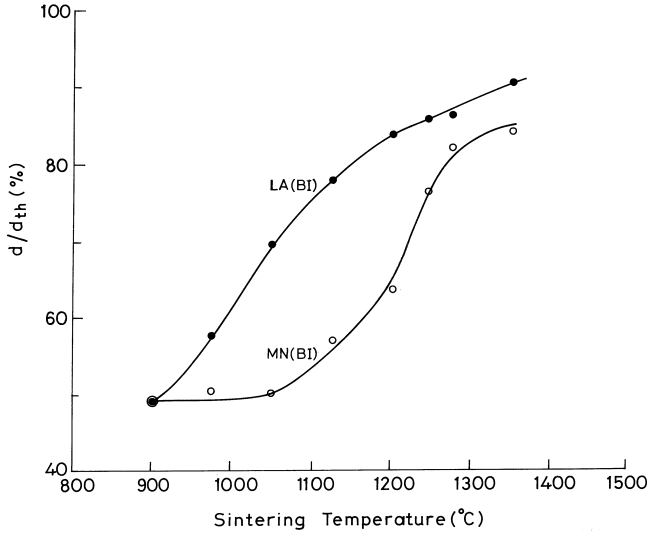

Fig. 8. Effect of sintering temperature on densification of the composition LA(BI) and MN(BI).

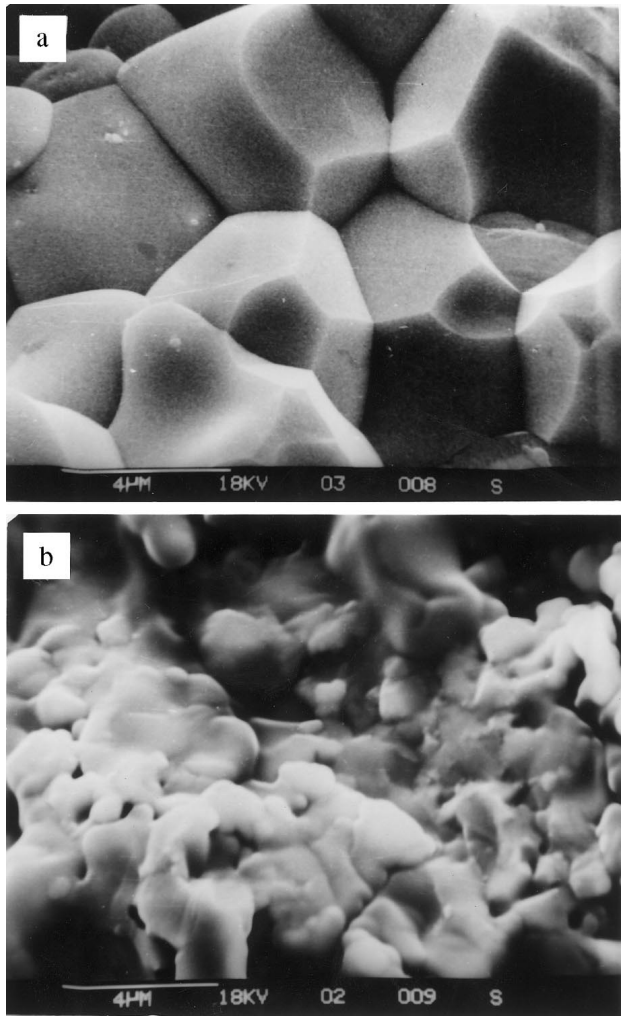

Fig. 9. SEM photographs of fractured surfaces of the sintered (1200°C for 6 h) sample of (a) LA(BI) and (b) MN(BI).

diffusivity of A site ions, which incidentally increases with the amount of Bi_2O_3 addition and thereby enhance the sintering process. A portion of Bi^{3+} evaporates during sintering which is evident from the results of chemical analysis (Table 1) and also from the earlier report [10]. Thus, in addition to "B" site vacancy, the vacancy created at A site increases the diffusivity of A site ions and hence enhance the sintering rate in the material. Stevenson et al. [9] also reported substantial improvement in the densification rate of manganites with a deficiency of A-site cations.

At around 1127°C, the upper limit of A:B site ratio for the stable compound comes down to 1.10 which is further reduced at 1200°C [16]. Addition of 10 wt% Bi_2O_3 just crosses this limit of forming a complete a

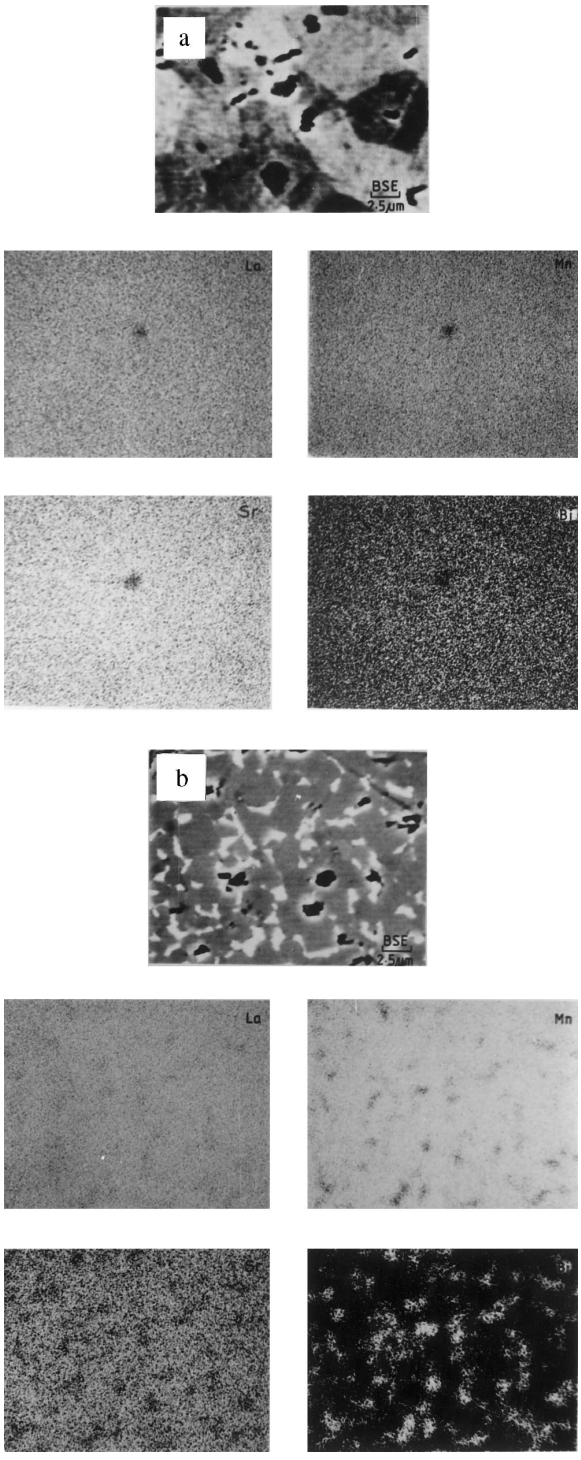

Fig. 10. EPMA photographs showing elemental distribution of the polished surface of sintered (1200°C for 6 h) sample of (a) LA(BI) and (b) MN(BI).

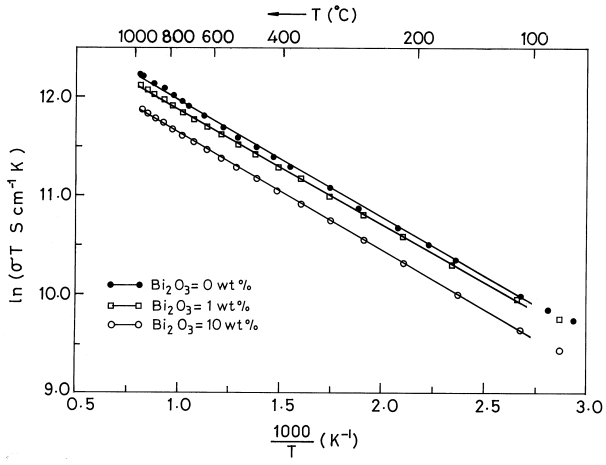

Fig. 11. Temperature dependence of electrical conductivity of sintered (1200°C for 6 h) pellets of $La_{0.84}Sr_{0.16}MnO_3$ containing different wt% of Bi_2O_3.

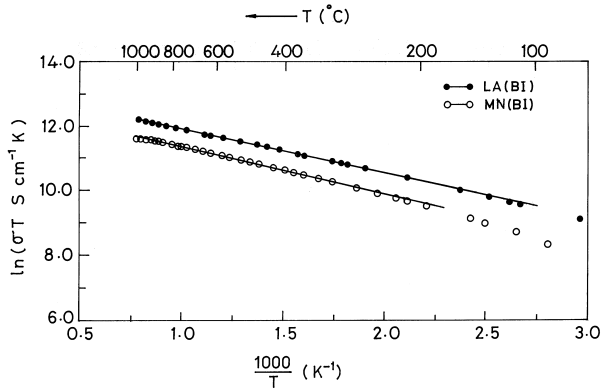

Fig. 12. Temperature dependence of electrical conductivity of LA(BI) sintered at 1200°C for 6 h and MN(BI) sintered at 1350°C for 6 h.

solid solution with $La(Sr)MnO_3$ (A:B = 1.11) at this temperature. The amount of bismuth evaporated at 1200°C is not sufficient to bring the ratio of A:B ions within the stability range at this temperature and therefore show a small amount of Bi rich secondary phase in EPMA study. This small amount of secondary phase is beyond the detection limit of XRD technique.

In case of composition LA(BI), the ratio of A:B ions becomes 1.00. Thus a single phase material is obtained within the calcination temperature of 850°C. Similar to previous compositions, here also the presence of Bi enhances the overall diffusivity of "A" site ions which increases further due to evaporation of some bismuth and consequently creation of "A" site vacancies at high temperatures. This increase in diffusivity of "A" site ions enhances the sintering rate of the material.

On the other hand, the actual ratio of A and B ions for the composition MN(BI) becomes 1.236, which is much beyond the limit of stability of perovskite phase and thus secondary phases containing A ions (oxides of lanthanum and bismuth) are observed from the XRD pattern of the material even when sintered at 1200°C. However, at a still higher sintering temperature of 1350°C most of the bismuth evaporates and the ratio of A:B ions comes down within the stability range giving rise to a single phase material. The enhancement in the

sintering process at higher temperature can also be explained from this consideration.

3.4. Electrical conductivity

The temperature dependence of electrical conductivity (σ) has been measured in the range 30–1000°C for all the samples of $La_{0.84}Sr_{0.16}MnO_3$ mixed with 1–10 wt% of Bi_2O_3 together with the compositions LA(BI) and MN(BI) all of which were sintered at 1200°C. The ln (σT) vs $1/T$ plots are presented in Fig. 11 for the samples without Bi_2O_3 and having Bi_2O_3 contents of 1 and 10 wt% (sintering temperature 1200°C). The conductivity value for the sample with 5 wt% Bi_2O_3 (not shown in figure) was found to be in between those of samples containing 1 and 10 wt% Bi_2O_3. Similar curves for the samples LA(BI) and MN(BI) sintered at 1200 and 1350°C, respectively are presented in Fig. 12. All these curves are straight lines over the entire range of temperature above T_c, metal–insulator transition temperature.

Table 2
Electrical conductivity, activation energy and thermal expansion coefficient of La(Sr)MnO_3 in presence of different Bi concentration

Bi_2O_3 content (wt%)	Activation energy, E_a (eV)	Conductivity at 1000°C σ_{1000} (S cm^{-1})	Thermal expansion coefficient (α) at 1000°C ($\times 10^{-6}$°C^{-1})
0	0.103	127	11.22
1	0.100	149	11.26
5	0.102	153	11.44
10	0.102	167	11.61
LA(BI)	0.118	161	—
MN(BI)	0.126	87	—

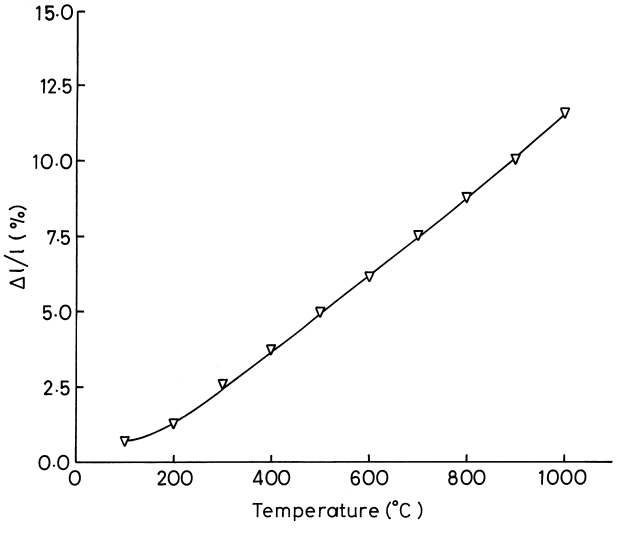

Fig. 13. Thermal expansion of $La_{0.84}Sr_{0.16}MnO_3$ (containing 10 wt% Bi_2O_3) vs temperature

The linearity in the plots is attributed to the thermally activated hopping of small polarons [10]. The electrical conductivity value at 1000°C for samples containing different amounts of Bi_2O_3 and also for the samples LA(BI) and MN(BI) together with the activation energies obtained from slope of the corresponding ln (σT) vs $1/T$ plots are presented in Table 2. The activation energies for the samples, having different Bi_2O_3, are nearly constant (Table 2) and almost equal to that obtained without using Bi_2O_3. However, the values obtained for the samples LA(BI) and MN(BI) (0.118 and 0.126 eV, respectively) are relatively high.

The increase in σ with Bi_2O_3 content (Fig. 12) may be attributed to the increase in density (d) of the material as reported earlier [6]. The electrical conductivity at 1000°C obtained for the sample without Bi_2O_3 and having a density of 88% of the theoretical value (sintering temperature 1350°C) is 160 S cm^{-1}. This is comparable to that obtained (167 S cm^{-1}) for the sample with 10 wt% Bi_2O_3, sintered at 1200°C and having a density of more than 93% of the theoretical value. These electrical conductivity data of Bi_2O_3 containing samples clearly indicate that addition of Bi_2O_3 does not have any deliterious effect on the electrical properties of the Sr-substituted $LaMnO_3$ while it has a significant effect on the sintering characteristics of the material.

3.5. Thermal expansion behaviour

The thermal expansion has also been measured for $La_{0.84}Sr_{0.16}MnO_3$ added with different Bi_2O_3 content and sintered at 1200°C for 6 h. Fig. 13 shows the relative thermal expansion vs temperature plot for the representative sample with 10 wt% Bi_2O_3. All the other samples have a similar type of behaviour. The thermal expansion coefficient at 1000°C increases only slightly with Bi_2O_3 content (Table 2).

4. Conclusions

Bi_2O_3 has been found to be a very effective sintering aid for La(Sr)MnO_3, particularly when the starting powder is prepared by autoignition route. In this case 10 wt% Bi_2O_3 addition lowers the sintering temperature by around 300°C. The enhancement in sintering is explained due to the solid solution of Bi_2O_3 with La(Sr)MnO_3 which increases the point defects in the lattice. Bi is found to go into the La site when substituted in La(Sr)MnO_3. If Bi is substituted for La, the material sinters at relatively low temperatures. However, when it is substituted for Mn, it does not go to the Mn site but remains as secondary phases and fails to enhance the sintering phenomenon. Bi_2O_3 addition does not affect significantly the physical properties like electrical conductivity and thermal expansion of the material.

Acknowledgement

Financial support by MNES, Government of India is gratefully acknowledged.

References

[1] F.J. Rohr, Solid Electrolytes, in: P. Hagenmuller, W. van Gool (Eds.), Academic Press, New York, 1978, p. 431.
[2] N.Q. Minh, Ceramic fuel cells, J. Am. Ceram. Soc. 76 (1993) 563–588.
[3] R. Von Helmolt, J. Wecker, B. Holzapfel, L. Schultz, K. Samwer, Giant negative magnetoresistance in perovskite $La_{2/3}Ba_{1/3}MnO_3$, Phys. Rev. Lett. 71 (1993) 2331–2333.
[4] R.J.H. Voorhoeve, J.P. Remeika, L.E. Trimble, A.S. Cooper, F.J. Disalvo, P.K. Gallagher, Perovskite-like $La_{1-x}K_xMnO_3$ and related compounds: solid state chemistry and the catalysis of the reduction of NO by CO and H_2, J. Solid State Chem. 14 (1975) 395–406.
[5] T. Arakawa, A. Yoshida, J. Shiokawa, The catalytic activity of rare earth manganites, Mat. Res. Bull. 15 (1980) 269–273.
[6] J.A.M. Van Roosmalen, J.P.P. Huijsmans, L. Plomp, Electrical conductivity in $La_{1-x}Sr_xMnO_{3+\delta}$, Solid State Ionics 66 (1993) 279–284.
[7] J.A.M. Van Roosmalen, E.H.P. Cordfunke, J.P.P. Huijsmans, Sinter behavior of $La(Sr)MnO_3$, Solid State Ionics 66 (1993) 285–293.
[8] K. Katayama, T. Ishihara, H. Ohta, S. Takeuchi, Y. Esaki, E. Inukai, Sintering and electrical conductivity of $La_{1-x}Sr_xMnO_3$, J. Ceram. Soc. Jpn. 97 (1989) 1324–1330.
[9] J.W. Stevenson, P.F. Hallman, T.R. Armstrong, L.A. Chick, Sintering behavior of doped lanthanum and yttrium manganite, J. Am. Ceram. Soc. 78 (1995) 507–512.
[10] M. Kertesz, I. Riess, D.S. Tannhauser, R. Langpape, F.J. Rohr, Structural and electrical conductivity of $La_{0.84}Sr_{0.16}MnO_3$, J. Solid State Chem. 42 (1982) 125–129.
[11] P. Kishan, D.R. Sagar, S.N. Chatterjee, L.K. Nagpaul, N. Kumar, K.K. Laroia, Optimization of Bi_2O_3 content and its role in sintering of lithium ferrites, in: F.Y. Wang (Ed.), Advances in Ceramics, vol.15, American Ceramic Society Westerville, OH, 1985, pp. 207–213.
[12] A. Chakraborty, P.S. Devi, S. Roy, H.S. Maiti, Low temperature synthesis of ultrafine $La_{0.84}Sr_{0.16}MnO_3$ powder by an autoignition process, J. Mater Res. 9 (1994) 986–991.
[13] A. Chakraborty, P.S. Devi, H.S. Maiti, Preparation of $La_{1-x}Sr_xMnO_3$ ($0 \leq - \leq 0.6$) powder by autoignition of carboxylate–nitrate gel, Mater. Lett. 20 (1994) 63–69.
[14] A. Chakraborty, P.S. Devi, H.S. Maiti, Low temperature synthesis and some physical properties of barium substituted lanthanum manganite ($La_{1-x}Ba_xMnO_3$), J. Mater. Res. 10 (1995) 918–925.
[15] D.W. Richerson, Modern Ceramic Engineering, 2nd. ed., Marcel Dekker, New York, 1992, p. 843.
[16] J.A.M. Van Roosmalen, P. Van Vlaanderen, E.H.P. Cordfunke, W.L. Ijdo, J.W. Ijdo, Phases in perovskite-type $LaMnO_{3+\delta}$ solid solution and the La_2O_3–Mn_2O_3 phase diagram, J. Solid State Chem. 114 (1995) 516–523.